



## STRESS-STRAIN MODEL OF HIGH-STRENGTH CONCRETE CONFINED BY RECTANGULAR TIES

Motoyuki SUZUKI<sup>1</sup>, Mitsuyoshi AKIYAMA<sup>2</sup>, Kee-Nam HONG<sup>3</sup>,  
Ian D. CAMERON<sup>4</sup> and Wei Lun WANG<sup>5</sup>

### SUMMARY

This paper presents a concentric loading test of square reinforced concrete columns confined by rectangular ties. Test variables include concrete compressive strength (45 to 130 MPa), tie yield strength (320 to 1300 MPa), and tie volumetric ratio (0.32 to 1.92%). It was confirmed that transverse reinforcement does not yield in columns using high-strength concrete or tie. A method to compute the stress in the transverse reinforcement at maximum concrete strength and a new stress-strain model for confined concrete are proposed. Over a wide range of confinement parameters, the model shows good correlation with stress-strain relationships established experimentally.

### INTRODUCTION

The confining pressure of confined concrete with normal-strength materials can be correctly calculated using the tie yield strength. However, depending on the confinement efficiency and grade of steel, the transverse reinforcement of columns using high-strength materials may or may not yield; we may not assume that lateral ties in poorly confined columns will yield. Additionally, test results and stress-strain models for poorly confined high-strength columns is rare, especially for columns with a tie volumetric ratio smaller than 2.0%, now the upper limit for RC bridge piers designed in Japan.

A total of 21 square RC columns were tested in this study. The following variables were evaluated for their effects on the stress-strain relationship of the confined concrete: concrete compressive strength, tie yield strength, and tie volumetric ratio. Relative to previous research [1]-[8], these specimens have smaller volumetric ratios. Based on the experimental results, a stress-strain model is proposed that is applicable to the wide range of test variables of this experiment.

### EXPERIMENTAL PROGRAM

#### Specimen Properties and Materials

<sup>1</sup> Professor, Tohoku university, Sendai, Japan, Email:suzuki@civil.tohoku.ac.jp

<sup>2</sup> Assistant Professor, Tohoku university, Sendai, Japan, Email:akiyama@civil.tohoku.ac.jp

<sup>3</sup> Graduate Student, Tohoku university, Sendai, Japan, Email:hong@design.civil.tohoku.ac.jp

<sup>4</sup> Exchange Student, University of Arizona, Tucson, AZ, USA, Email:cameroni@u.arizona.edu

<sup>5</sup> Graduate Student, Tohoku university, Sendai, Japan, Email: wang@design.civil.tohoku.ac.jp

**Table 1. Specimen details**

Notation of specimens	$\sigma_c'$ <sup>1)</sup> (MPa)	Transverse reinforcement					
		Diameter	Spacing $s$	Volumetric ratio $\rho_s$	Yield strength $f_{sy}$ <sup>2)</sup>	$\rho_s \cdot f_{sy}$	
SF1P0Y0-1 SF1P0Y0-2 SF1P0Y0-3	46.3	—	—	—	—	—	
SF1P1Y3		6.4 mm	25 mm	1.92%	1288 MPa	24.7 MPa	
SF1P2Y1		6.0 mm	50 mm	1.01%	317 MPa	3.20 MPa	
SF1P2Y3		6.4 mm	50 mm	0.96%	1288 MPa	12.4 MPa	
SF1P3Y1		6.0 mm	100 mm	0.51%	317 MPa	1.62 MPa	
SF1P3Y2		6.0 mm	100 mm	0.51%	1028 MPa	5.24 MPa	
SF1P3Y3		6.4 mm	100 mm	0.48%	1288 MPa	6.18 MPa	
SF1P4Y3		6.4 mm	150 mm	0.32%	1288 MPa	4.12 MPa	
SF2P0Y0-1 SF2P0Y0-2 SF2P0Y0-3		84.8	—	—	—	—	—
SF2P1Y3			6.4 mm	25 mm	1.92%	1288 MPa	24.7 MPa
SF2P2Y1	6.0 mm		50 mm	1.01%	317 MPa	3.20 MPa	
SF2P2Y3	6.4 mm		50 mm	0.96%	1288 MPa	12.4 MPa	
SF2P3Y1	6.0 mm		100 mm	0.51%	317 MPa	1.62 MPa	
SF2P3Y2	6.0 mm		100 mm	0.51%	1028 MPa	5.24 MPa	
SF2P3Y3	6.4 mm		100 mm	0.48%	1288 MPa	6.18 MPa	
SF2P4Y3	6.4 mm		150 mm	0.32%	1288 MPa	4.12 MPa	
SF3P0Y0-1 SF3P0Y0-2 SF3P0Y0-3	128		—	—	—	—	—
SF3P1Y3			6.4 mm	25 mm	1.92%	1288 MPa	24.7 MPa
SF3P2Y1		6.0 mm	50 mm	1.01%	317 MPa	3.20 MPa	
SF3P2Y3		6.4 mm	50 mm	0.96%	1288 MPa	12.4 MPa	
SF3P3Y1		6.0 mm	100 mm	0.51%	317 MPa	1.62 MPa	
SF3P3Y2		6.0 mm	100 mm	0.51%	1028 MPa	5.24 MPa	
SF3P3Y3		6.4 mm	100 mm	0.48%	1288 MPa	6.18 MPa	
SF3P4Y3		6.4 mm	150 mm	0.32%	1288 MPa	4.12 MPa	

<sup>1)</sup> The average compressive strength obtained from test of three standard cylinder ( $\phi 100 \times 200$ mm)

<sup>2)</sup> The average yield strength obtained from three specimens

All tested specimens were 250 mm  $\times$  250 mm square sections, 750 mm in height. The test parameters included concrete compressive strength (46.3, 84.8, 128 MPa), tie volumetric ratio (0.32~1.92%), and yield strength of transverse reinforcement (317, 1028, 1288MPa). Specimen details are listed in Table 1. SD295 was used as longitudinal reinforcement in all specimens. Three different grades of steel (317, 1028, 1288 MPa) were used for lateral reinforcement. The diameter of the lateral reinforcement was approximately 6 mm (see Table 1 for more detail). In all confined specimens, the spacing of transverse reinforcement was reduced to 15 mm in the end regions to provide extra confinement and to ensure that failure occurred near

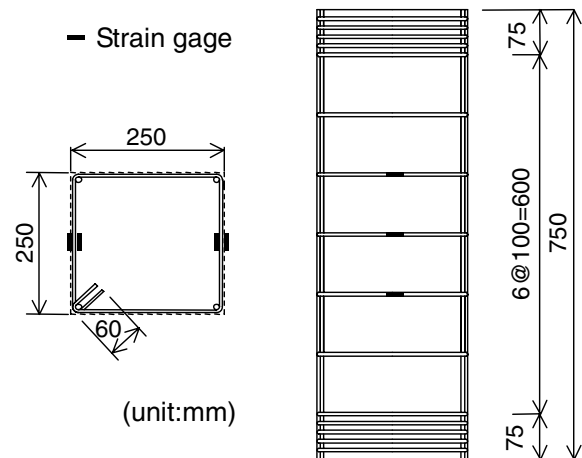


**Fig. 1. Details of Test Specimen**

the center of the specimen. All lateral ties were anchored by 135-degree hooks around one of the longitudinal bars, extending 60 mm into the concrete core. A schematic of a sample arrangement ( $s=100$  mm) is given in Fig. 1.

For each concrete strength, three standard cylinders ( $\phi 100$  mm  $\times$  200 mm) were tested to determine the average compressive strength ( $\sigma'_{c}$ , given in Table 1). Also, three columns for each batch of concrete (e.g. SF1PY0-1) were prepared as unconfined concrete specimens to establish the in-place concrete strength ( $\sigma'_{c0}$ ). For this study, all test specimens were designed without cover concrete for two reasons: (1) in specimens with wide tie spacing, the loss of load-carrying capacity resulting from the spalling of cover concrete can cause sudden column failure; and (2) if the load-carrying capacity of cover is correctly subtracted from the load, the cover does not affect the evaluation of confined concrete [9],[10].

The specimens were cast from three batches, one for each target strength. In the following sections, these batches are referred to by their SF group number, to facilitate reference to the specimens of a single concrete strength: SF1,  $\sigma'_{c}=46.3$  MPa; SF2,  $\sigma'_{c}=84.8$  MPa; and SF3,  $\sigma'_{c}=128$  MPa. For a uniform distribution of the load during testing, it is important that the top and bottom faces of a column are parallel. Specimens were cast horizontally to ensure this.

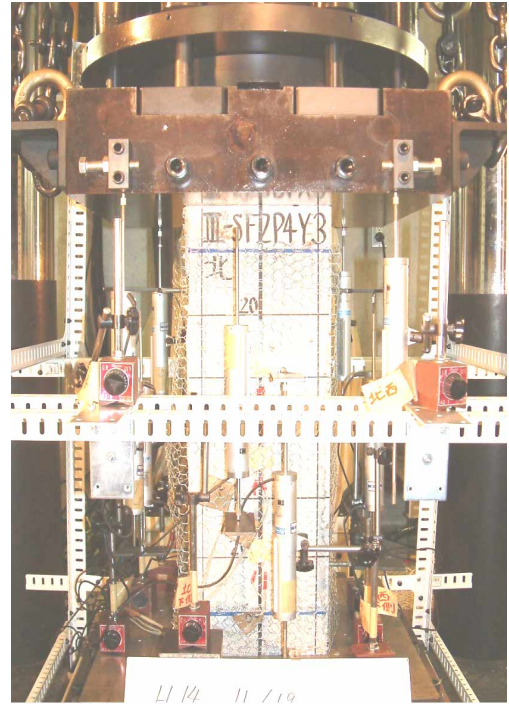


**Fig. 2. Test Specimen Set Up**

### **Instrumentation and Testing Procedure**

A concentric vertical load was applied using a 10MN-capacity hydraulic universal testing machine. An overall view of test specimen set up is shown in Fig. 2. It is generally accepted that high strength concrete should be tested in a very rigid machine [8], [11]. The steel reaction columns of the machine used in this research are stiff enough to meet such requirements and permit the machine to load at a rate as low as 0.01mm/min.

The axial deformation of the specimens was recorded using four linear variable differential transformers (LVDTs) located at each corner of the specimen. They were attached to the platen and crosshead for a gage length of 750 mm. The overall concrete axial strain was calculated as the average of the LVDT measurements divided by the gage length. Steel strain measurements were made by electrical resistance strain gages bonded to the transverse reinforcement. Cracking, buckling of axial reinforcement, and other observational data were also recorded during all tests.

## **TEST RESULT**

### **Failure Mode**

For each concrete strength, three unconfined specimens were tested in order to obtain the average unconfined concrete compressive strength ( $\sigma'_{c0}$ ). The maximum concrete stress in confined columns is termed  $\sigma_{cc}$ . The strength gain ratio of a confined specimen is one measurement of the confinement effect, defined as the ratio of these strengths, i.e.  $\sigma_{cc}/\sigma'_{c0} > 1$ .

For the specimens of SF1, the minimum strength gain ratio was 1.02 (SF1P4Y3,  $\rho_s=0.32\%$ ), while the maximum was 1.40 (SF1P1Y3,  $\rho_s=1.92\%$ ). When peak strength was reached, vertical cracking occurred between tie bars. No new damage appeared after maximum strength. In the specimen having the closest spacing of transverse reinforcement (SF1P1Y3), stress decreased very slowly after peak strength, and the core concrete was almost undamaged (see Fig. 3(a)). With the widest tie bar spacing, the damage to specimen SF1P4Y3 (Fig. 3(b)) was concentrated between tie bars, and its core concrete was significantly reduced due to significant buckling of longitudinal reinforcement. Additionally, for all SF1 specimens, the lateral ties bowed out due to the expansion of the core concrete (see Fig. 4(a)).

The strength gain ratio of SF2 specimens was a minimum of 1.07 (SF2P4Y3,  $\rho_s=0.32\%$ ) and a maximum of 1.31 (SF2P1Y3,  $\rho_s=1.92\%$ ). Although these SF2 specimens cracked in the same way as the specimens of SF1, these specimens showed a more rapid reduction in load-carrying capacity after peak strength. Comparing equally confined specimens from these two groups, we find that when tie spacing is close, the damage to the core is similar and slight (compare Figs 3(a) and (c)). On the other hand, when tie spacing is wide, the core of the SF2 column is damaged more seriously than that of the SF1 column. Also, the failure of the SF2 specimens was relatively sudden and explosive.

The strength gain ratio of SF3 specimens ( $\sigma'_c=128\text{MPa}$ ) was a minimum of 1.07 (SF3P4Y3,  $\rho_s=0.32\%$ ) and a maximum of 1.31 (SF3P1Y3,  $\rho_s=1.92\%$ ). All specimens of SF3 exhibited brittle failure. Except for SF3P1Y3, all specimens lost load resistance with almost no strain gain after peak strength. Compared to specimens of SF2 and SF3 with the same spacing, the damage to specimen SF3P1Y3 was concentrated in the narrower region between ties. A well-defined shear failure plane, attaining the full length of the specimen, was formed in the SF3 specimens where  $\rho_s < 0.51\%$ . This failure pattern depends on lateral confining pressure and therefore volumetric ratio: when lateral confining pressure is low, the angle between the specimen axis and plane of shear failure becomes smaller [2]. Finally, the lateral expansion of core concrete and bowing of lateral ties was unobservable in SF3 (see Fig. 4(b)).

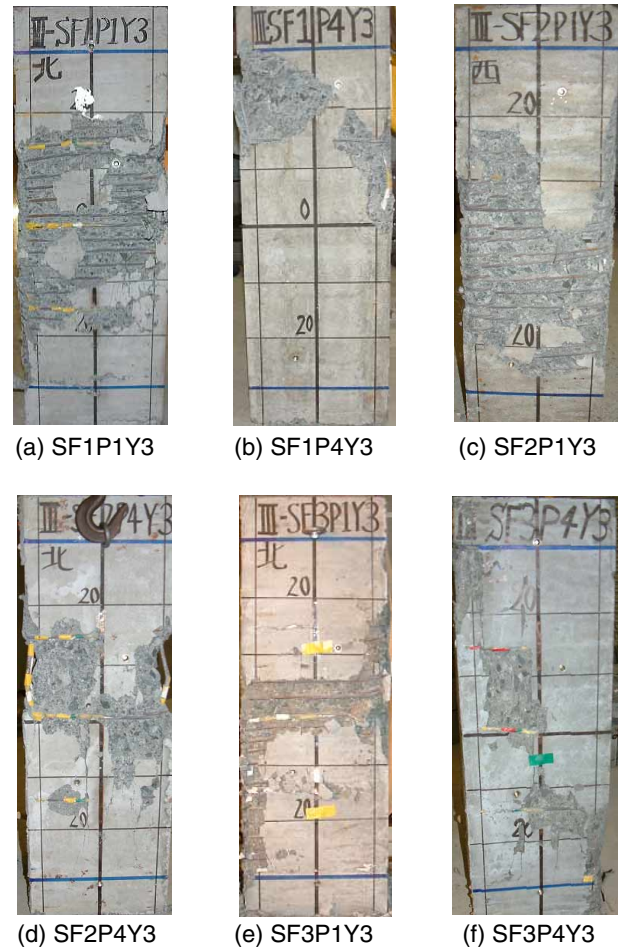


Fig. 3. Specimens after Testing

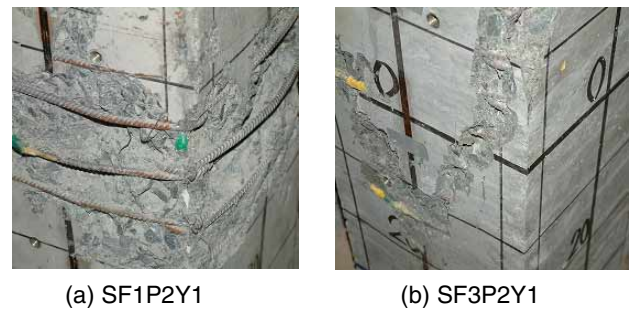


Fig. 4. Difference of Confinement Effect

## Discussion of Test Results

### *Effect of volumetric ratio of transverse reinforcement*

Fig. 5 compares the stress-strain curves of specimens between which only volumetric ratio of transverse reinforcement ( $\rho_s$ ) differs. The tie yield strength ( $f_{sy}$ ) for all these specimens is 1288 MPa. It is clear that  $\sigma_{cc}/\sigma'_{c0}$  is proportionally related to  $\rho_s$ : as volumetric ratio  $\rho_s$  increases, the peak stress and the corresponding strain of confined concrete increases. However, with the same  $\rho_s$ , columns made of high-strength concrete experience a smaller strength gain ratio than columns with normal-strength concrete.

With additional lateral reinforcement, SF1 and SF2 columns exhibit greater ductility. But, a consistent decrease in ductility is observed with increasing concrete strength. This is because high-strength concrete exhibits less lateral expansion under axial compression than normal-strength concrete due to its higher modulus of elasticity and its lower internal micro cracking [1], [12]. Since confining pressure is developed when transverse reinforcement restrains the lateral expansion of concrete, the confining reinforcement comes into play later when loading high-strength concrete. Consequently, passive confinement is less efficient in high-strength concrete.

For example, SF3 columns lost at least 50% of load-carrying capacity almost immediately after the peak strength. This occurs even when  $\rho_s=1.92\%$ , which is near the maximum  $\rho_s$  allowed in RC bridge piers designed in Japan. At approximately 1/3 of their peak strength, specimens with lower volumetric ratios lost capacity so quickly that the machine was unable to continue loading.

### *Effect of yield strength of transverse reinforcement*

Fig. 6 shows the stress-strain curves for specimens having different tie yield strengths, but with similar volumetric ratios ( $\rho_s \approx 0.5\%$ ). It is clear that increasing the yield strength does not significantly improve the confinement effect. Fig. 7 compares stress-strain curves for specimens of varying  $\rho_s$  and  $f_{sy}$ . They are grouped according to concrete strength, but

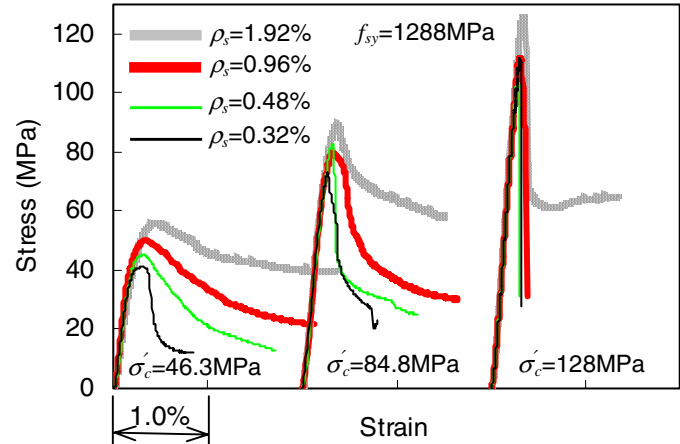


**Fig. 5. Effect of Tie Volumetric Ratio**

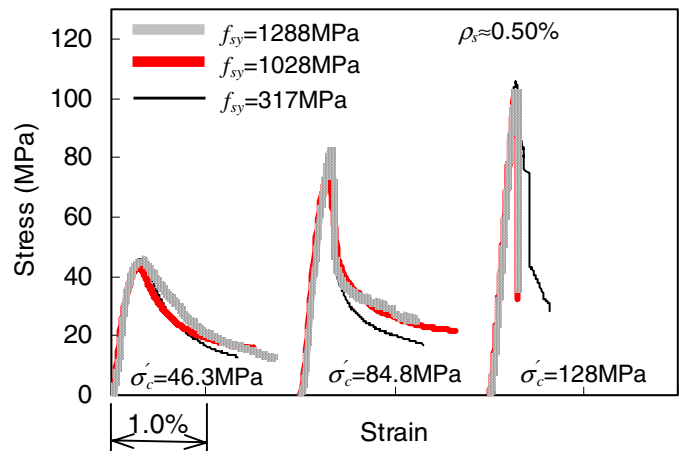


**Fig. 6. Effect of Tie Yield Strength**

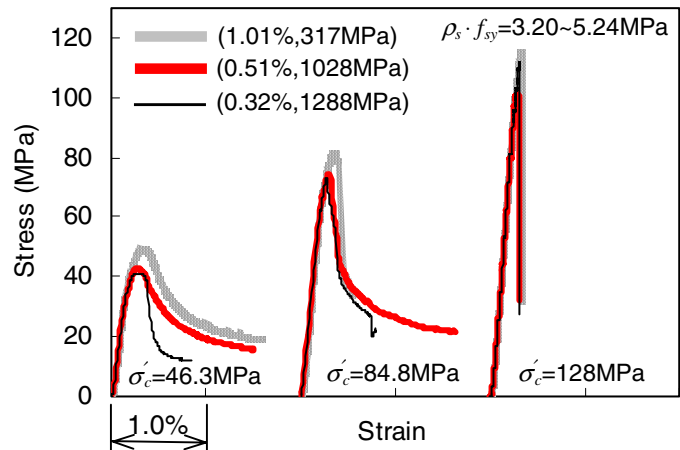


**Fig. 7. Effect of  $\rho_s \cdot f_{sy}$**

only specimens with  $\rho_s \cdot f_{sy}$  in the range of 3.20~5.24 MPa are presented. Even when columns have approximately the same  $\rho_s \cdot f_{sy}$  product, those with higher volumetric ratios of lower-grade steel performed better than those with lower volumetric ratios of higher-grade steel. This suggests that increasing the grade of transverse reinforcement cannot make up for a proportional reduction in the volumetric ratio.

These phenomena can be explained by Fig. 8, which shows how the ratio  $f_{s,exp}/f_{sy}$  varies with both tie and concrete strength. Here,  $f_{s,exp}$  is the tensile stress in the transverse reinforcement at peak concrete stress, averaged from all of the sample's strain gage measurements. Fig. 8 shows that: i) when  $f_{sy}=317$  MPa (except SF3 columns), transverse reinforcement yields at peak concrete strength; ii) even if  $f_{sy}=1028$  and 1288 MPa,  $f_{s,exp}/f_{sy}$  is 0.41 or less; and iii) the transverse reinforcement does not yield in any SF3 specimens.

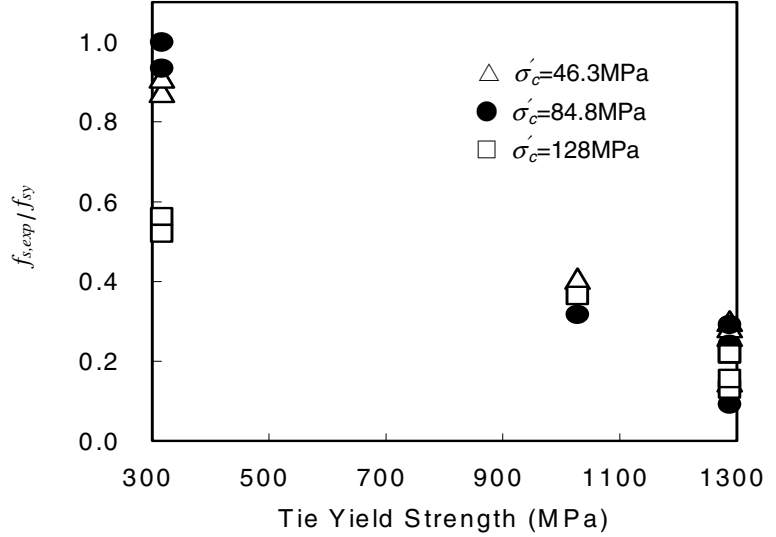


**Fig. 8. Stress in the Tie Bar at Peak Strength**

Lateral confining pressure is typically calculated using the tie yield strength, predicting higher confinement pressures when higher grade steel is used. However, these experiments show that high-grade tie bar does not yield in high-strength concrete. Therefore, the tie yield strength cannot be used when calculating the confinement pressure, and confinement calculations using  $f_{sy}$  will overestimate the lateral confining pressure. Thus, the behavior shown in Figs. 6 and 7 is to be expected.

## STRESS-STRAIN MODEL

### Formulation of Confinement Effect

In this study, the effective confinement index was defined as the effective lateral pressure ( $p_e$ ) calculated from Eq. (1).

$$p_e = k_e \rho_w f_{s,c} \quad (1)$$

where  $\rho_w$  is the area ratio of transverse reinforcement;  $f_{s,c}$  is the stress in the transverse reinforcement at the peak strength (see next section); and  $k_e$  is the effective confinement coefficient [13] given by

$$k_e = \left(1 - \sum \frac{(w_i')^2}{6b_c d_c}\right) \left(1 - \frac{s'}{2b_c}\right) \left(1 - \frac{s'}{2d_c}\right) / (1 - \rho_{cc}) \quad (2)$$

where  $w_i$  is the clear spacing between adjacent longitudinal steel bars in a rectangular section;  $s'$  is the clear spacing of ties;  $b_c$  and  $d_c$  are the widths of the concrete core; and  $\rho_{cc}$  is the longitudinal reinforcement ratio in the core section.  $E_{des}$  was defined as the slope of the straight line connecting the point of the peak strength and the point at which the stress drops to 85% of the peak strength.

A regression analysis was performed on all test results to formulate the peak strength ( $\sigma_{cc}$ ), the strain at peak strength ( $\epsilon_{cc}$ ), and the slope of the descending branch ( $E_{des}$ ) in terms of  $p_e$ . The results of regression analyses are presented in Eqs. (3)-(5), respectively.

$$\frac{\sigma_{cc}}{\sigma_{c0}} = 1.0 + 4.1 \left( \frac{p_e}{\sigma_{c0}} \right)^{0.70} \quad (3)$$

$$\varepsilon_{cc} = \varepsilon_{c0} + 0.015 \left( \frac{p_e}{\sigma_{c0}} \right)^{0.56} \quad (4)$$

$$E_{des} = 0.026 \frac{\sigma_{c0}^3}{p_e^{0.4}} \quad (5)$$

$$\sigma_{c0} = 0.85 \sigma_c' \quad (6)$$

$$\varepsilon_{c0} = 0.0028 - 0.0008 k_3 \quad (7)$$

$$k_3 = 40 / \sigma_{c0} \leq 1.0 \quad (8)$$

where  $p_e$ ,  $\sigma_{c0}$ , and  $E_{des}$  are in MPa;  $\sigma_{c0}$  and  $\varepsilon_{cc}$  are the peak stress and corresponding strain of unconfined concrete.

### Stress in Transverse Reinforcement at Peak Strength

In this section, the relationship between the lateral confining pressure and lateral strain is simplified, and a method for calculating the stress  $f_{s,c}$  in the transverse reinforcement at the peak strength of confined concrete is presented.

Nielsen [14], after collecting data from previous triaxial compression experiments on concrete ranging from 40 to 110 MPa, reported that the lateral strain and axial strain at the maximum stress are related by

$$\varepsilon_{cc} = -2.2 \varepsilon_{3,p} \quad (9)$$

where compression is positive. This formula holds under a wide range of confinement pressures and concrete strengths ( $0 < p/\sigma_c' < 2.0$ ).

The stress  $f_{s,c}$  in the transverse reinforcement at the peak strength of confined concrete can be computed with the following iterative procedure:

- i) Using Eq. (1), calculate the effective confinement pressure  $p_e$ , assuming  $f_{s,c} = f_{sy}$ .
- ii) Estimate the lateral concrete strain  $\varepsilon_{3,p}$  with Eqs. (4) and (9).
- iii) Assuming that the strain in the lateral tie is equal to  $\varepsilon_{3,p}$ , evaluate the resulting stress  $f_{s,c}$  using the stress-strain curve of the steel ties.
- iv) If  $f_{s,c} < f_{sy}$ , recalculate the effective confinement pressure ( $p_e$ ) with the new value of  $f_{s,c}$ .
- v) Repeat steps ii)~iv) until the value of  $f_{s,c}$  converges.

To evaluate the accuracy of this method, the ratio  $f_{s,exp} / f_{s,c}$  was studied; it has an average value of 0.98 and a 22% coefficient of variation. Finally, a formula for  $f_{s,c}$  (Eq. (10)) was derived from a regression analysis of the parameters related to the iterative procedure.

$$f_{s,c} = E_s \left\{ 0.45 \varepsilon_{c0} + 0.73 \left( \frac{k_e \rho_w}{\sigma_{c0}} \right)^{0.70} \right\} \leq f_{sy} \quad (10)$$

where  $E_s$  is modulus of elasticity of transverse reinforcement and  $\sigma_{c0}$  is in MPa. Using Eq. (10),  $f_{s,c}$  can be calculated to a sufficient degree of accuracy. Therefore,  $f_{s,c}$ ,  $p_e$ , and other modeling parameters can be computed without iteration.

### Proposed Stress-Strain model

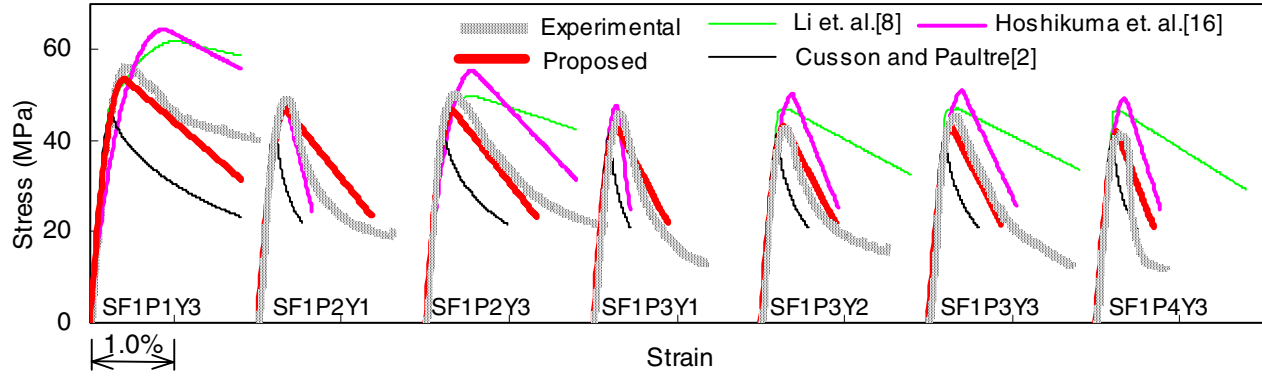


Fig. 9. Comparison of Stress-Strain Models ( $\sigma'_c=46.3$  MPa)

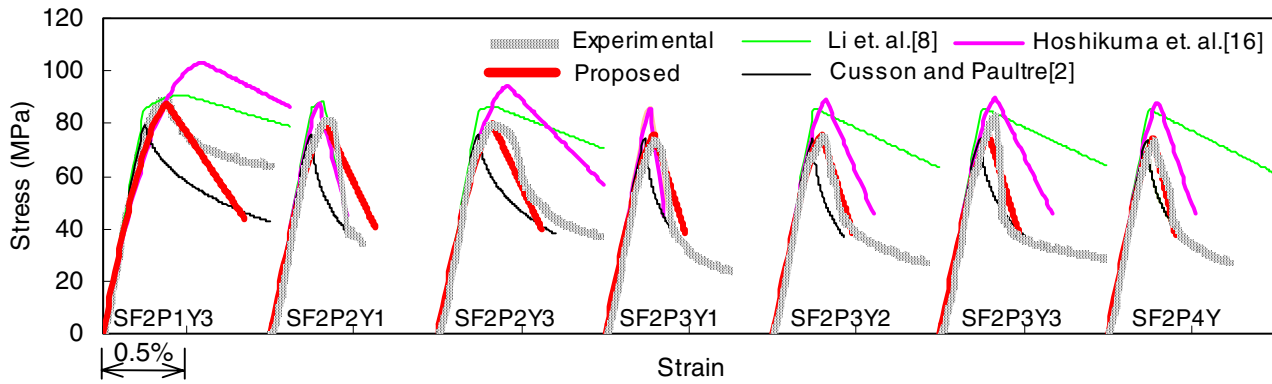


Fig. 10. Comparison of Stress-Strain Models ( $\sigma'_c=84.8$  MPa)

#### Stress-strain relation

$\sigma_{cc}$ ,  $\epsilon_{cc}$ , and  $E_{des}$  can be calculated with Eqs. (3)-(5). Based on the formulation of this confinement effect, a stress-strain model is proposed that is applicable to the wide range of test variables of this experiment.

Many researchers have modeled the ascending branch of a stress-strain curve of confined concrete. First, the adaptability of previous ascending branch models was examined. In order to produce the best correlation, the stress-strain model of Fafitis and Shah [15] was used, where the initial Young's modulus of the concrete was calculated using a formula by Razvi and Saatcioglu [3] Eq. (13).

Eqs. (11)-(14) are proposed as the stress-strain model that is applicable to the wide range of test variables of this experiment.

$$\sigma_c = \sigma_{cc} \left\{ 1 - \left( 1 - \frac{\epsilon_c}{\epsilon_{cc}} \right)^\alpha \right\} \quad (0 \leq \epsilon_c \leq \epsilon_{cc}) \quad (11)$$

$$\alpha = E_c \frac{\epsilon_{cc}}{\sigma_{cc}} \quad (12)$$

$$E_c = 3320\sqrt{\sigma_{c0}} + 6900 \quad (13)$$

$$\sigma_c = \sigma_{cc} - E_{des}(\epsilon_c - \epsilon_{cc}) \quad (\epsilon_{cc} \leq \epsilon_c) \quad (14)$$

where  $\sigma_{cc}$  is in MPa.

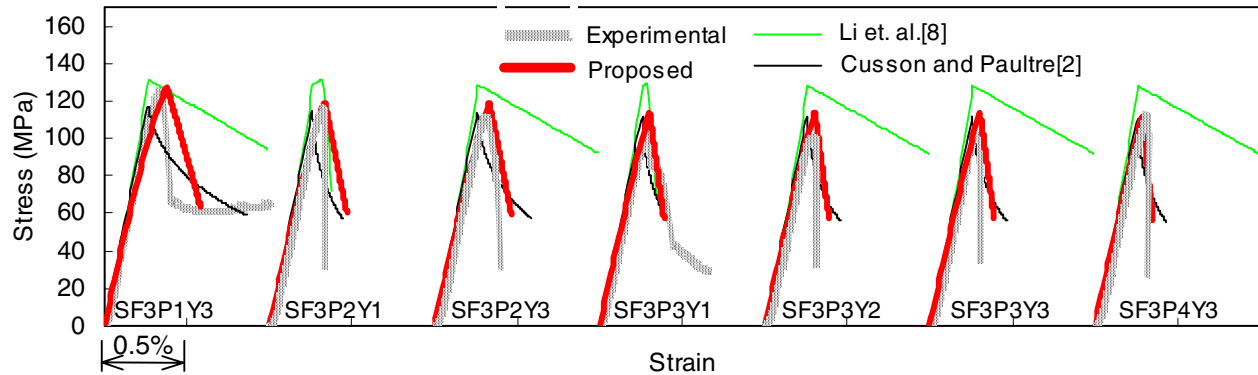


**Fig. 11. Comparison of Stress-Strain Models ( $\sigma'_c=128$  MPa)**

#### *Comparison of proposed model*

The comparison of the model to the experiment results of all 21 confined specimens is shown in Figs. 9-11. Curves obtained from the models of Cusson and Paultre [2], Li et al. [8], and Hoshikuma et al. [16] are also shown in each figure. All models shown in Figs. 9-11 were developed using the axial strain of similar specimens: square columns with a height to width ratio of approximately 3.0. In all cases, the stress-strain relation proposed by this research accurately reproduces the experiment result. Having used  $f_{s,c}$  instead of  $f_{sy}$  in the calculation of confinement pressure, even the phenomena seen in Figs. 6-7 is successfully reproduced.

Previous models show good agreement with columns similar to those tested in their respective experiments. For example, the Hoshikuma model, proposed for normal-strength concrete and smaller tie yield strength, predicts the behavior of specimens SF1P2Y1 and SF1P3Y1. Furthermore, if normal-strength steel tie is used, the results of SF2 specimens ( $\sigma'_c=84.8$  MPa) can also be predicted with sufficient accuracy using this model. However, since the Hoshikuma and Li models use the tie yield strength as the stress in the transverse reinforcement, they overestimate the peak strength and strain of specimens where  $f_{sy}=1028$  and 1288 MPa. On the other hand, since many of Cusson and Paultre's specimens were made of concrete stronger than 90 MPa, their model generally underestimates the results of SF1 and 2 specimens.

## CONCLUSIONS

The following conclusions can be drawn from the combined experimental and analytical research in this paper:

1) 21 square RC columns were tested, with concrete compressive strengths ranging from 45 to 130 MPa and transverse reinforcement of yield strengths ranging from 320 to 1300 MPa. We find from experiment that: high-strength columns exhibit i) less lateral expansion under axial compression than normal-strength columns, and bowing of lateral ties in these specimens does not occur; and ii) a plane of shear failure, attaining the full length of the specimen, was formed in specimens with smaller tie volumetric ratios.

2) It was confirmed that: i) increasing the tie yield strength does not significantly improve the confinement effect; ii) even if columns have approximately the same  $\rho_s \cdot f_{sy}$  product, those with higher volumetric ratios of lower-grade steel performed better than those with lower volumetric ratios of higher-grade steel; and iii) this is because, when higher strength ties are used, the stress in the transverse reinforcement at peak concrete strength is less than 50% of the tie yield strength.

3) Based on results from the 21 columns tested in this study, a stress-strain model was proposed. This model offers several advantages: no iterative calculations are required, and the same model accurately predicts results for columns with both normal- and high-strength materials.

## REFERENCES

1. Cusson, D. and Paultre, P., "High-Strength Concrete Columns Confined by Rectangular Ties," *Journal of Structural Engineering, ASCE*, Vol.120, No.3, pp.783-804, 1994.
2. Cusson, D. and Paultre, P., "Stress-Strain Model for Confined High-Strength Concrete," *Journal of Structural Engineering, ASCE*, Vol.121, No.3, pp.468-477, 1995.
3. Razvi, S. and Saatcioglu, M., "Confinement Model for High-Strength Concrete," *Journal of Structural Engineering, ASCE*, Vol.125, No.3, pp.281-289, 1999.
4. Razvi, S. and Saatcioglu, M., "Circular High-Strength Concrete Columns under Concentric Compression," *ACI Structural Journal*, Vol. 96, No.5, pp.817-825, 1999.
5. Saatcioglu, M. and Razvi, S., "High-Strength Concrete Columns with Square Sections under Concentric Compression," *Journal of Structural Engineering, ASCE*, Vol.124, No.12, pp.1438-1447, 1998.
6. Nagashima, T., Sugano, S., Kimura, H. and Ichikawa, A., "Monotonic Axial Compression Test on Ultra-High-Strength Concrete Tied Columns," *10th World Conference on Earthquake Engineering*, pp.2983-2988, 1992.
7. Itakura, Y. and Yagenji, A., "Compressive Test on High-Strength R/C Columns and their Analysis Based on Energy Concept," *10th World Conference on Earthquake Engineering*, pp.2599-2602, 1992.
8. Li Bing, Park, R. and Tanaka, H., "Stress-Strain Behavior of High-Strength Concrete Confined by Ultra-High- and Normal-Strength Transverse Reinforcements," *ACI Structural Journal*, Vol. 98, No.3, pp.395-406, 2001.
9. Sakino, K. and Sun, Y. P., "Axial Behavior of Confined High Strength Concrete," *Proceedings of the Japan Concrete Institute*, Vol.15, No.2, pp.713-718, 1993. (In Japanese)
10. Sun, Y. P. and Sakino, K., "Ductility Improvement of Reinforced Concrete Column with High Strength Materials," *Proceedings of the Japan Concrete Institute*, Vol.15, No.2, pp.719-729, 1993. (In Japanese)
11. Tomosawa, F., Noguchi, T., and Onoyama, K., "Effect of Longitudinal of Testing Machine on Compressive Strength of Concrete," *Proceedings of the Japan Concrete Institute*, Vol.12, No.1, pp.251-256, 1990. (In Japanese)
12. Fujita, M., Sato, R., Matsumoto, K., and Takaki, Y., "Size Effect on Shear Strength of RC Beams Using HSC without Shear Reinforcement," *Journal of Materials, Concrete Structures and Pavements, JSCE*, No.711/V-56, pp.161-172, 2002. (In Japanese)
13. Mander, J. B., Priestley, M., J., N. and Park., R., "Theoretical Stress-Strain Model for Confined Concrete," *Journal of Structural Engineering, ASCE*, Vol.114, No.8, pp.1804-1826, 1988.
14. Nielsen, C. V., "Triaxial Behavior of High-Strength Concrete and Mortar," *ACI Materials Journal*, Vol.95, No.2, pp.144-151, 1998.
15. Fafitis, A. and Shah, S. P., "Lateral Reinforcement for High- Strength Concrete Columns," *High-Strength Concrete, SP-87, ACI, Detroit, Mich.*, pp.213-232, 1985.
16. Hoshikuma, J., Kawashima, K., and Nagaya, K., "A Stress-Strain Model for Reinforced Concrete Columns Confined by Lateral Reinforcement," *Journal of Materials, Concrete Structures and Pavements, JSCE*, No.520/V-28, pp.1-11, 1995. (In Japanese)